4 Representations of the Electromagnetic Field

4.1 Basics

A quantum mechanical state is completely described by its density matrix ρ. The density matrix ρ can be expanded in different basises $\{|\psi\rangle\}$:

$$\rho = \sum_{i,j} D_{ij} |\psi_i\rangle \langle\psi_j| \qquad \text{for a discrete set of basis states} \qquad (158)$$

The c-number matrix $D_{ij} = \langle\psi_i| \rho |\psi_j\rangle$ is a representation of the density operator.

One example is the *number state or Fock state representation* of the density matrix.

$$\rho_{nm} = \sum_{n,m} P_{nm} |n\rangle \langle m| \qquad (159)$$

The diagonal elements in the Fock representation give the probability to find exactly n photons in the field!

A trivial example is the density matrix of a Fock State $|k\rangle$:

$$\rho = |k\rangle \langle k| \quad \text{and } \rho_{nm} = \delta_{nk}\delta_{km} \qquad (160)$$

Another example is the density matrix of a thermal state of a free single mode field:

$$\rho = \frac{\exp[-\hbar\omega a^+ a/k_b T]}{Tr\{\exp[-\hbar\omega a^+ a/k_b T]\}} \qquad (161)$$

In the Fock representation the matrix is:

$$\rho = \sum_n \exp[-\hbar\omega n/k_b T][1 - \exp(-\hbar\omega/k_b T)] |n\rangle \langle n| \qquad (162)$$

$$= \sum_n \frac{\langle n\rangle^n}{(1 + \langle n\rangle)^{n+1}} |n\rangle \langle n| \qquad (163)$$

with

$$\langle n\rangle = Tr(a^+ a\rho) = [\exp(\hbar\omega/k_b T) - 1]^{-1} \qquad (164)$$

This leads to the well-known Bose-Einstein distribution:

$$\rho_{nn} = \langle n| \rho |n\rangle = P_n = \frac{\langle n\rangle^n}{(1 + \langle n\rangle)^{n+1}} \tag{165}$$

4.2   Glauber-Sudarshan or P-representation

The P-representation is an expansion in a coherent state basis $|\{\alpha\}\rangle$:

$$\rho = \int P(\alpha, \alpha^*) |\alpha\rangle \langle\alpha|\ d^2\alpha \tag{166}$$

A trivial example is again the P-representation of a coherent state $|\alpha\rangle$, which is simply the delta function $\delta(\alpha - a')$.

The P-representation of a thermal state is a Gaussian:

$$P(\alpha) = \frac{1}{\pi\bar{n}}e^{-|\alpha|^2/\bar{n}} \tag{167}$$

Again it follows:

$$P_n = \langle n| \rho |n\rangle = \int P(\alpha, \alpha^*) |\langle n|\alpha\rangle|^2\ d^2\alpha \tag{168}$$

$$= \frac{1}{\pi\bar{n}} \int e^{-|\alpha|^2/\bar{n}}\frac{|\alpha|^{2n}}{n!}e^{-|\alpha|^2}\ d^2\alpha \tag{169}$$

The last integral can be evaluated and gives again the thermal distribution:

$$P_n = \frac{\langle n\rangle^n}{(1 + \langle n\rangle)^{n+1}} \tag{170}$$

4.3   Optical Equivalence Theorem

Why is the P-representation useful?

- $|\alpha\rangle$ corresponds to a classical state.

- The expectation values of normally ordered operator functions are similiar to their classical counterpart.

38

Let $g^{(N)}$ be a normally ordered operator function (i.e., all creation operators left, all annihilation operators right):

$$g^{(N)} = \sum_{n,m} c_{nm}(a^+)^n a^m \tag{171}$$

The expectation value of $g^{(N)}$ is:

$$\left\langle g^{(N)} \right\rangle = Tr[\rho g^{(N)}(a^+, a)] \tag{172}$$

$$= Tr \left\{ \int P(\alpha) |\alpha\rangle \langle\alpha| \sum_{n,m} c_{nm}(a^+)^n a^m \ d^2\alpha \right\} \tag{173}$$

$$= \int P(\alpha) \sum_{n,m} c_{nm} \langle\alpha| (a^+)^n a^m |\alpha\rangle \ d^2\alpha \tag{174}$$

$$= \int P(\alpha) \sum_{n,m} c_{nm}(\alpha^*)^n \alpha^m \ d^2\alpha \tag{175}$$

$$= \int P(\alpha) g^{(N)}(\alpha, \alpha^*) \ d^2\alpha \tag{176}$$

The last row gives the classical average value of the c-number function $g^{(N)}(\alpha, \alpha^*)$ wheighted be the c-number function $P(\alpha)$. Formally one can write

$$\left\langle g^{(N)}(a, a^+) \right\rangle = \left\langle g^{(N)}(\alpha, \alpha^*) \right\rangle_P \tag{177}$$

This is the optical equivalence theorem.

Example: The $g^{(2)}$ function:
Classically:

$$g^{(2)}(0) = \frac{\langle a^+ a^+ a a \rangle}{\langle a^+ a \rangle^2} \geq 1 \tag{178}$$

Using the optical equivalence theorem the numerator of the expression above is

$$\int P(\alpha) \left(|\alpha|^2\right)^2 \ d^2\alpha \geq \left(\int P(\alpha) |\alpha|^2 \ d^2\alpha \right)^2 = \left\langle |\alpha|^2 \right\rangle^2 \tag{179}$$

$$\Leftrightarrow \tag{180}$$

$$\int P(\alpha) \left(\left(|\alpha|^2\right)^2 - \left\langle |\alpha|^2 \right\rangle^2 \right) \ d^2\alpha = \int P(\alpha) Var(\alpha) \ d^2\alpha \geq 0 \tag{181}$$

But, we have seen that $g^{(2)}(0)$ can be smaller than 1 in some cases! Thus:

$$\int P(\alpha) Var(\alpha) \ d^2\alpha < 0 \qquad \text{for some cases} \tag{182}$$

Since $Var(\alpha)$ is a positive function, $P(\alpha)$ has to be negative for some cases. Thus, $P(\alpha)$ cannot be interpreted as a probability function!

For this reason $P(\alpha)$ and other functions are referred to as *quasi-probability functions*. For non-classical field states the quasi-probability functions can have negative values!

4.4 Wigner Function

The first quasi-probability function was introduced by Wigner in 1932.

The so-called Wigner function or Wigner distribution can be derived from the P-distribution via convolution with a Gaussian:

$$W(\alpha) = \frac{2}{\pi} \int_{-\infty}^{\infty} P(\beta) \exp\left[-2|\beta - \alpha|^2\right] \, d^2\beta \tag{183}$$

It is easy to show that $W(\alpha)$ can be written in terms of the conjugate variables $q = \alpha + \alpha^*$ and $p = -i(\alpha - \alpha^*)$

$$W(q, p) = \frac{1}{4\pi} \int_{-\infty}^{\infty} \langle q + q' | \rho | q - q' \rangle \exp\left(\frac{iq'p}{2}\right) \, dq' \tag{184}$$

$W(q, p)$ is the quasi-probability distribution of the conjugate variables q, p.

From the Wigner function the probability density $\Pr(q)$ and $\Pr(p)$ of both q and p can be derived via integration:

$$\Pr(q) = \int_{-\infty}^{\infty} W(q, p) \, dp \tag{185}$$

$$= \frac{1}{4\pi} \int_{-\infty}^{\infty} \langle q + q' | \rho | q - q' \rangle \, dq' \int_{-\infty}^{\infty} \exp\left(\frac{iq'p}{2}\right) \, dp \tag{186}$$

$$= \frac{1}{4\pi} \int_{-\infty}^{\infty} \langle q + q' | \rho | q - q' \rangle \, 4\pi\delta(q') \, dq' \tag{187}$$

$$= \langle q | \rho | q \rangle \tag{188}$$

$$= \psi^*(q)\psi(q) = |\psi(q)|^2 \quad \text{for a pure state} \tag{189}$$

Similar:

$$\Pr(p) = \int_{-\infty}^{\infty} W(q,p) \; dq = \langle p | \rho | p \rangle \tag{190}$$

Examples for Wigner functions are: Wigner function of a coherent state:

$$W_{coherent} = \frac{2}{\pi} \exp\left[-\frac{1}{2}\left(q^2 + p^2\right)\right] \tag{191}$$

Wigner function of a Fock state:

$$W_n = \frac{2}{\pi}(-1)^n L_n\left[4(q^2 + p^2)\right] e^{-2(q^2+p^2)} \tag{192}$$

The following pictures show the Wigner functions of a coherent state and a single photon Fock-state. The non-classical character of the Fock-state shows up as a negativity of the Wigner function at the origin.

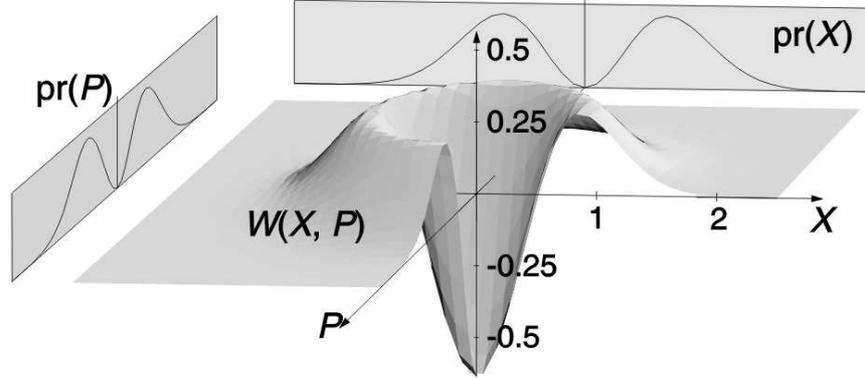Figure 19: Wigner function of a harmonic oscillator eigenstate.

Figure 20: Wigner function of a single photon Fock state [from Lvovsky et al., Phys. Rev. Lett. 87, 050402 (2001)]

4.5 Quantum Tomography

The Wigner function can be projected on any axis (not only on the p- and q-axis).

The probability distribution along an arbitrary axis is:

$$\Pr(q, \vartheta) = \int_{-\infty}^{\infty} W(q \cos \vartheta - p \sin \vartheta, q \sin \vartheta + p \cos \vartheta) \; dp \tag{193}$$

The Wigner function and thus the complete information of the state ρ can be reconstructed by measuring $\Pr(q, \vartheta)$ for all possible ϑ.

For the special case of a rotationally symmetric Wigner function one finds:

$$W(r) = -\frac{1}{\pi} \int_{0}^{\infty} \frac{\frac{d}{dq} \Pr(q)}{q^2 - r^2} \; dq \tag{194}$$

A more complex transformation holds for the general case. Such a reconstruction of the Wigner function is called *quantum state tomography*.

How can one measure the probability distribution $Pr(q)$?

One way to do this is using *homodyne detection*. A typical homodyne experiment is shown in the following picture:
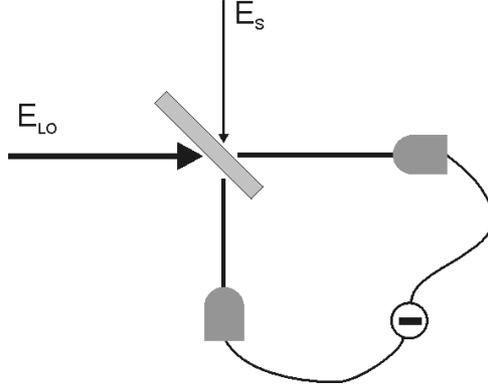
42

Figure 21: Principle of homodyne detection.

We assume single mode fields in both arms of the input. One arm is called the *local oscillator*. It contains a strong field which we assume to be classical:

$$E_{LO} \propto E_{LO}^{(0)} \, \alpha + c.c \quad \text{where } \alpha \text{ is a c-number} \tag{195}$$

The other input arms contains a weak quantum field, the *signal field*:

$$E_S \propto E_S^{(0)} \, a_S + h.c. \tag{196}$$

The two photodetectors detect (positive frequency part only!) in arm 1 or 2:

$$I_{1,2} = \left\langle E_{1,2}^+ E_{1,2} \right\rangle = \frac{1}{2} \left\langle (E_{LO} \pm E_S)^+ (E_{LO} \pm E_S) \right\rangle \tag{197}$$

$$= \frac{1}{2} \left\{ \left\langle E_S^+ E_S^+ \right\rangle + \left\langle E_{LO}^+ E_{LO}^+ \right\rangle \pm \left\langle E_S^{(0)} a E_{LO}^{(0)} \alpha + E_S^{(0)} a^+ E_{LO}^{(0)} \alpha^* \right\rangle \right\} \tag{198}$$

$$= \frac{1}{2} \left\{ \left\langle I_S \right\rangle + \left\langle I_{LO} \right\rangle \pm E_S^{(0)} E_{LO}^{(0)} |\alpha| \left\langle a e^{i\vartheta} + a^+ e^{-i\vartheta} \right\rangle \right\} \tag{199}$$

Thus, the difference of the detected intensity (measured, e.g., as a difference in the photo current) is:

$$I_1 - I_2 = E_S^{(0)} E_{LO}^{(0)} |\alpha| \left\langle a e^{i\vartheta} + a^+ e^{-i\vartheta} \right\rangle \tag{200}$$

$$= E_S^{(0)} E_{LO}^{(0)} |\alpha| \left\langle q(\vartheta) \right\rangle \tag{201}$$

The homodyne detection measures the amplified (by the large amplitude of the classical field $|\alpha|$) expectation value of the quadrature component $q(\vartheta)$. The phase ϑ can be changed very easily by changing the field of the classical field, e.g., by a delay line.

Thus, plotting the difference of $\langle q(\vartheta) \rangle_T$ versus the time gives $Pr(q(\vartheta))$ and from the measurement of $Pr(q(\vartheta))$ for many different ϑ the Wigner function can be derived.

$Pr(q(\vartheta))$ is also called the marginal distribution.

4.6   Tomography of a Single Photon Fock State

Fock-states are non-classical states. However, it is very difficult to create them.

It is important to divide single photon Fock states $|1\rangle$ from the more general class of single photon states $|\psi_1\rangle$.

We may define a single photon state as a state of the form

$$|\psi_1\rangle = \sum_{\{n\}} c_{\{n\}} |\{n\}\rangle = \sum_k c_k a_k^+ |\{0\}\rangle \tag{202}$$

where for all the n-tupel $\{n\}$ there is only one n_i different from 0, e.g., $|n\rangle_j = |000...1...\rangle$. The single photon Fock-state is a special case (only one specific k is relevant).

Such as state can be created by:

- Spontaneous decay of a single two level system

- Detection of one of the photons from an entangled photon pair (e.g., from parametric down-conversion)

If such a single photon (state) is detected with a photodetector, the photocurrent is proportional to

$$\Psi_1 = \langle 0| E^{(+)}(r,t) |\psi_1\rangle \tag{203}$$

We will see in a later chapter that for a detector at a distance r from a spontaneously decaying atom:

$$\Psi_1 = \frac{A_0}{r} \Theta(t - \frac{r}{c}) e^{-i(t-r/c)(\omega - i\Gamma/2)} \tag{204}$$

where Θ is the step function, which accounts for the finite speed of light.

The rate Γ is the rate of spontaneous exponential decay of the upper state of the atom. The frequency spectrum (which is proportional to $G^{(1)}(\tau)$) has a Lorentzian shape and thus a non-zero width.

A single photon state is usually a superposition of many spatial and spectral modes!

In the experiment by Lvovsky et al. (Phys. Rev. Lett. 87, 050402 (2001)) a single photon state was created by projecting one of the photons of a parametric pair. In this case the set of spatial and spectral filters in the detection arm determines the state in the other arm. In order to perform a subsequent tomography via homodyning this state had to be matched as good as possible to the local oscillator state.

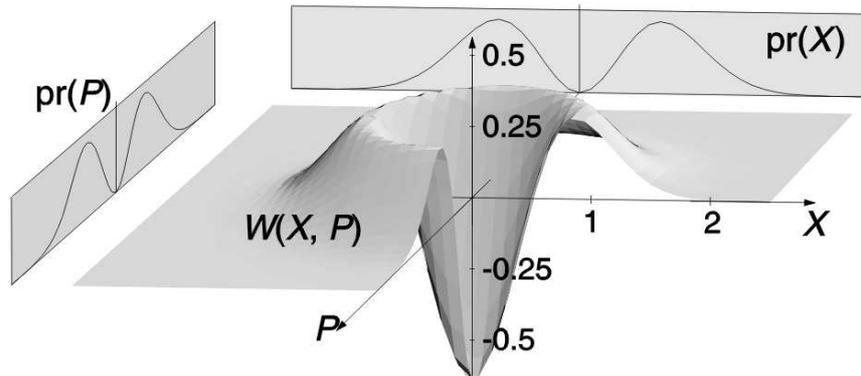The following picture shows again the Wigner function of a single photon Fock state:

Figure 22: Wigner function of a single photon Fock state [from Lvovsky et al., Phys. Rev. Lett. 87, 050402 (2001)]

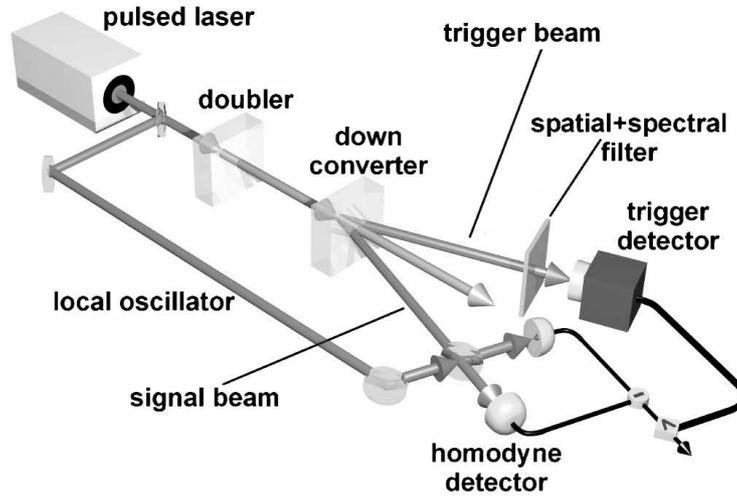The next picture shows the experimental setup used in the tomography experiment:

Figure 23: [from Lvovsky et al., Phys. Rev. Lett. 87, 050402 (2001)]

A crucial point in a tomography experiment is the overall efficiency (combined effect of detection efficiency, spectral matching, mode matching, fluctuations etc.). If this is too low the results of the tomography approach the measurement of a vacuum state.
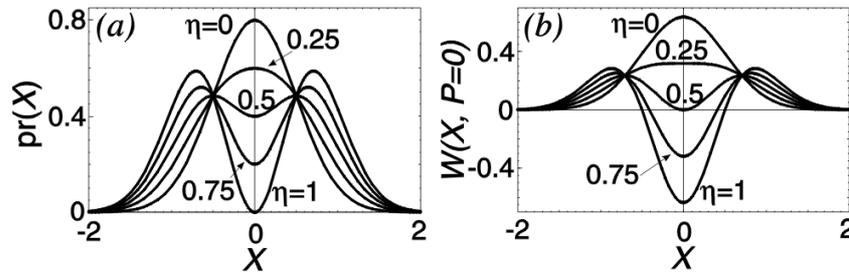

Figure 24: Marginal distribution (left) and reconstructed Wigner function for different efficiencies η [from Lvovsky et al., Phys. Rev. Lett. 87, 050402 (2001)]

In the experiment the marginal distribution is measured. From the marginal distribution the Wigner function can be reconstructed. The experimental results clearly show a negativity of the Wigner function, and thus, the non-classical character of

the detected light. Also the strong admixture of the vacuum state can be seen in the reconstructed diagonal elements of the density matrix.

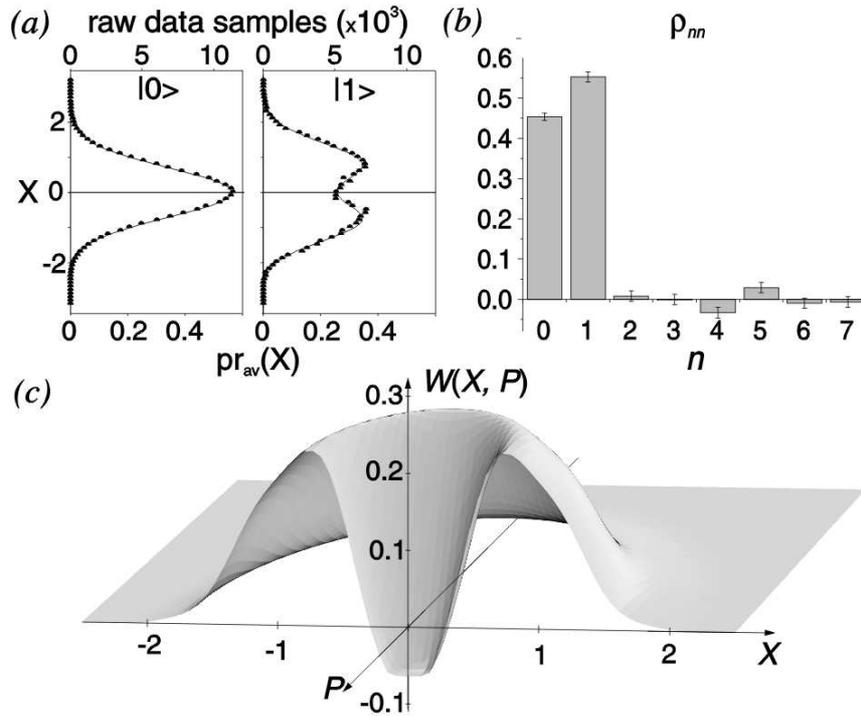The experimental data is summarized in the following picture:

Figure 25: Marginal distrubutions of the vaccum and single photon state (a), reconstructed diagonal of the density matrix (b), and reconstructed density matrix (c) [from Lvovsky et al., Phys. Rev. Lett. 87, 050402 (2001)]